A&A 449, 127–134 (2006)
DOI: 10.1051/0004-6361:20053770
© ESO 2006

Astronomy & Astrophysics

Chemical abundances of 32 mildly metal-poor stars⋆

H. W. Zhang[1] and G. Zhao[2]

[1] Department of Astronomy, School of Physics, Peking University, Beijing 100871, PR China
e-mail: zhw@bac.pku.edu.cn
[2] National Astronomical Observatories, Chinese Academy of Sciences, Beijing 100012, PR China

Received 22 July 2005 / Accepted 26 October 2005

ABSTRACT

Context. The formation scenario of the Galactic thick disk is an unresolved problem. Chemical abundances in long-lived dwarf stars of the thin and thick disks provide information of the Galactic disk formation.
Aims. We present photospheric abundances of the O, Na, Mg, Al, Si, Ca, Sc, Ti, V, Cr, Mn, Ni, and Ba elements for 32 mildly metal-poor stars with [Fe/H] ~ -0.7. According to their kinematics, age, and [α/Fe], sample stars are identified to thin disk, thick disk, and halo population memberships. Element abundances for sample stars are discussed as a function of metallicity.
Methods. High resolution and high signal-to-noise ratio spectra were obtained with the Coudé Echelle Spectrograph mounted on the 2.16 m telescope at the National Astronomical Observatories (Xinglong, China). Effective temperatures were estimated from colour indices, and surface gravities from Hipparcos parallaxes. Stellar abundances were determined from a differential LTE analysis. The kinematics parameters were calculated from the parallax, proper motion, and radial velocity. Stellar ages were determined from theoretical stellar evolution tracks.
Results. The average age of the thick disk stars is older than the thin disk stars. Our element abundance results extend and confirm previous works. The oxygen and other α-elements (Mg, Si, Ca, and Ti) abundances of thin and thick disk stars show distinct trends at [Fe/H] ≤ -0.60. The [Al/Fe] behaviour is exactly as an α-element, although the separation for [Na/Fe] of thin and thick disk stars is not clear. The elements V, Cr, and Ni follow Fe very closely, and there is no offset between thin and thick disk stars, but the Sc and Mn abundance trends of the thin and thick disk stars are different, and [Ba/Fe] of thin disk and thick disk stars shows different behaviour.

Key words. stars: abundances – stars: kinematics – Galaxy: disk

1. Introduction

The existence of a population of stars with kinematics, ages, and chemical abundances that lie between the characteristic values for the halo and the disk populations is a long-standing problem in studies of Galactic structure and evolution.

Observational works from the 1980's showed that Galaxy as having two disk-like components: the thin and the thick disks (Gilmore & Reid 1983). The formation scenario of the Galactic thick disk is still unresolved (Majewski 1993). There are essentially two major formation scenarios for the Galactic thick disk: (i) the pre-thin disk (top-down) models, where the formation of the thick disk precedes the formation of the thin disk; and (ii) the post-thin disk (bottom-up) models, where the thick disk is the result of some action on or by the thin disk. Much more work on stellar ages, kinematics, and abundances has to be carried out before we can be certain about the basic scenario for the formation and evolution of our Galaxy.

The study of chemical abundance in long-lived dwarf stars of the thin and thick disks provides information about the Galactic disk formation and has become an active research area in recent years. A strong indication of the Galactic thin and thick disks as discrete populations with respect to kinematics and age comes from Edvardsson et al. (1993). The following works show systematic differences between the chemical composition of the thin and thick disk stars: Fuhrmann (1998, 2004), Gratton et al. (2000), Prochaska et al. (2000), Mashonkina & Gehren (2001), Reddy et al. (2003), Gehren et al. (2004, 2005), Brewer & Carney (2005). Recently, Bensby et al. (2003, 2004, 2005) selected two samples with a high kinematical probability of belonging to either the thin and thick disk and found distinct abundance trends at sub-solar metallicities. For a comprehensive review, the reader is referred to Nissen (2003).

Chen et al. (2000) studied the chemical composition of 90 F and G dwarf stars, and do not find any clear [α/Fe] separation between thin and thick stars. As pointed out by Prochaska et al. (2000), this may, however, be due to the fact that they selected dwarf stars in the temperature range 5800 K $< T_{\rm eff} <$ 6400 K. Hence, the old thick disk stars with $T_{\rm eff} <$ 5700 K were not included.

In order to extend the work of Chen et al. (2000), we study a sample of candidates of thick disk stars. In this paper the

⋆ Tables 1 and 3 are only available in electronic form at the CDS via anonymous ftp to cdsarc.u-strasbg.fr (130.79.128.5) or via http://cdsweb.u-strasbg.fr/cgi-bin/qcat?J/A+A/449/127

Article published by EDP Sciences and available at http://www.edpsciences.org/aa or http://dx.doi.org/10.1051/0004-6361:20053770

results of 32 mildly metal-poor stars with [Fe/H] ~ -0.7 are presented. In Sect. 2 we describe the observation and the data reduction, and in Sect. 3 the abundance determination. In Sect. 4 we determine the kinematic parameter, age, and population membership of sample stars. In Sect. 5 we discuss the abundance trends with metallicity, conclusions followed by in the last section.

2. Observation and data reduction

The observation was performed on 10 nights during 1999 using the Coudé Echelle Spectrograph attached to the 2.16 m telescope at the National Astronomical Observatories (Xinglong, China). The red arm of the spectrograph with a 31.6 grooves/mm grating was used in combination with a prism as cross-disperser, thus providing a good separation for the different echelle orders. With a 0.5 mm slit (~1.06″), the resolving power was 37 000 in the middle-focus camera system. The detector was a Tek CCD (1024 × 1024 pixels with $24 \times 24\ \mu m^2$ each in size). The signal-to-noise ratio of spectra at 6400 Å was about 150 pixel^{-1}. The wavelength coverage was from 5600 Å to 8300 Å with some gaps. A detailed description of the technical aspects of the spectrograph can be found in Zhao & Li (2001). During the observation run, some spectra of bright, rapidly rotating, spectral-type B stars were observed. These spectra were used to remove the telluric O_2 features.

A reduction of two-dimensional echelle spectral data was performed using the ESO-MIDAS[1] software package. The data reduction includes locating the echelle order on the multi-order two-dimensional spectrum, subtracting the background, and extracting the orders by summation along the slit. The pixel-to-pixel variation was corrected by dividing with a flatfield taken at the same night. The wavelength calibration was based on a thorium-argon lamp. The radial velocities were measured from about 20 intermediately strong and unblended lines with an accuracy of 1.5 km s^{-1}. The spectra were then normalized by a continuum function determined by fitting a spline curve to a set of pre-selected continuum windows (typically 20–30 per order) taken from the solar atlas.

The equivalent widths (EWs) were measured by direct integration and Gaussian fitting, depending on which method gave the best fit of the line profile. The EWs of all lines are given in Table 1. The accuracy of the EWs was estimated by comparing them to the independent measurements by Chen et al. (2000) for the 9 stars we have in common, which is shown in Fig. 1. The systematic difference between the two sets of measurements is small, and a linear least squares fitting gives:

$$EW(\text{this work}) = (0.986 \pm 0.010)\, EW(\text{Chen et al.}) + (0.96 \pm 0.37). \quad (1)$$

The standard deviations around the relation are 5.0 mÅ (for 676 lines in common with Chen et al. 2000). We estimate an rms error of about 3 mÅ in our EWs.

[1] ESO-MIDAS is the acronym for the European Southern Observatory Munich Image Data Analysis System, which is developed and maintained by the European Southern Observatory.

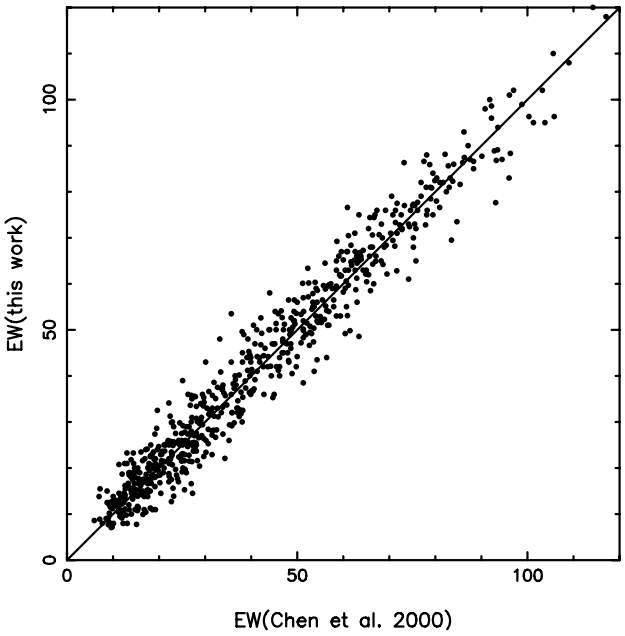

Fig. 1. A comparison of equivalent widths measured in this work with those in Chen et al. (2000) for 9 stars in common.

3. Abundance determination

3.1. Atmospheric parameters

The effective temperature was determined from the $b - y$ and $V - K$ colour indices using the IRFM calibrations of Alonso et al. (1996). According to the discussion in Nissen et al. (2004), the error in the effective temperature is expected to be around 70 K. With the effective temperature and absolute magnitude, the stellar mass was then determined from the star's position in the $M_v - \log T_{\rm eff}$ diagram by interpolating the evolutionary tracks of VandenBerg et al. (2000). The surface gravity was calculated from Hipparcos parallax (ESA 1997) using the method described in Chen et al. (2000). We estimated that the error of log g is about 0.10 dex. The microturbulence (ξ_t) was obtained by requiring a zero slope of [Fe/H] vs. EW.

The whole procedure of deriving $T_{\rm eff}$, $\log g$, and ξ_t was iterated to consistency when spectroscopic [Fe/H] was obtained. The stellar parameters of sample stars are given in Table 2.

3.2. Abundance analysis

The abundance analysis was based on a net of flux constant, homogeneous, LTE model atmospheres interpolated from the extensive grids in Kurucz (1993). With the code ABONTEST8, which was kindly provided by Dr. Pierre Magain, abundances were derived by requiring that the calculated equivalent width from the model should match the observed one.

The details for line selection, atomic line data, calculation of the uncertainties, and the contribution from systematic errors are the same as those discussed in Chen et al. (2000). Solar abundances, calculated from the daylight spectrum, were used to derive stellar abundances relative to solar values. As expected, errors are around 0.05 dex for relative abundance, [X/Fe], and of the order of 0.10 dex for [Fe/H]. Finally,

Table 2. Stellar parameters of sample stars.

Name	$T_{\rm eff}$ [K]	log g [cm s^{-2}]	[Fe/H] [dex]	$\xi_{\rm t}$ [km s^{-1}]	Mass [$M_\odot$]
HD 3454	6081.	4.22	–0.59	1.40	0.98
HD 6834	6369.	4.07	–0.64	1.56	1.08
BD+29 366	5652.	4.29	–0.99	1.49	0.74
HD 18768	5712.	3.84	–0.61	1.42	1.08
HD 22879	5778.	4.25	–0.84	1.06	0.77
HD 25173	5898.	3.94	–0.63	1.45	1.04
HD 28474	5682.	4.29	–0.73	1.56	0.74
HD 45205	5826.	4.07	–0.93	1.73	0.85
HD 49732	6232.	4.12	–0.74	1.66	1.03
HD 59374	5756.	4.31	–0.97	1.02	0.71
HD 59984A	5883.	3.92	–0.76	1.56	1.00
HD 62301	5845.	4.08	–0.69	1.33	0.90
HD 64385	5827.	4.13	–0.81	1.50	0.86
HD 76932	5869.	4.06	–0.88	1.29	0.80
HD 94028	5916.	4.18	–1.40	1.33	0.67
HD101606A	6194.	3.75	–0.68	1.71	1.16
HD 105755	5709.	3.99	–0.78	1.62	0.79
HD 106516A	6146.	4.31	–0.76	1.40	0.97
HD 108076	5675.	4.43	–0.87	1.03	0.80
HD 114762	5808.	4.13	–0.80	1.55	0.87
HD 157089	5716.	4.04	–0.70	1.69	0.92
HD 189558	5667.	3.80	–1.11	1.36	0.88
HD 194598	5962.	4.22	–0.99	0.94	0.72
HD 195633	5990.	3.79	–0.62	1.48	1.01
HD 200580	5780.	3.92	–0.69	1.70	1.02
HD 201889	5615.	4.00	–0.84	1.29	0.75
HD 204155	5773.	3.99	–0.67	1.14	0.81
HD 207978	6324.	4.04	–0.62	1.89	1.13
HD 215257	5873.	4.18	–0.73	1.31	0.91
HD 216385	6232.	3.90	–0.26	1.69	1.19
HD 219617	5912.	3.84	–1.42	1.42	0.82
HD 221377A	6308.	3.77	–0.80	2.19	1.05

the abundances of the Fe, O, Mg, Si, Ca, Ti, Na, Al, Sc, V, Cr, Mn, Ni, Ba elements of 32 sample stars are given in Table 3.

3.3. Comparison with other studies

We compared our results with recent studies that have some stars in common with ours. We found 9 stars in our sample are common to Chen et al. (2000), 5 stars to Bensby et al. (2003, 2005), and 4 stars to Reddy et al. (2003). The results of these comparisons are displayed in Table 4. We note that there is close agreement over the adopted atmospheric parameters and derived abundances.

4. Kinematic properties, age, and population membership

4.1. Kinematic parameters

The space velocities (U, V, W) and orbital parameters ($R_{\rm max}$, $R_{\rm min}$, $Z_{\rm max}$, e) are calculated from the Hipparcos parallax, proper motion, and radial velocity that we measured.

Calculation of the space velocity with respect to the Sun is based on the method presented by Johnson & Soderblom (1987). The correction of space velocity to the local standard of rest (LSR) is $(-10.0, +5.2, +7.2)$ km s^{-1} in (U, V, W), as derived by Dehnen & Binney (1998). The rotational velocity of the LSR with respect to the Galaxy is set to 225.2 km s^{-1} and the galactocentric distance is set to 8.5 kpc. The numerical integration of the Galactic orbits is done by adopting the Galactic mass model of Allen & Santillan (1991). A detailed discussion can be found in Zhang & Zhao (2005).

Table 4. Average differences in atmospheric parameters and abundances.

Quantity	Chen −ours	σ	Bensby −ours	σ	Reddy −ours	σ
$T_{\rm eff}$	5	49	91	105	–5	55
log g	0.15	0.20	0.03	0.04	0.01	0.10
$\xi_{\rm t}$	0.25	0.29	–0.06	0.30	0.03	0.13
[Fe/H]	0.03	0.06	0.04	0.07	0.05	0.09
[α/Fe]	–0.05	0.04	–0.03	0.05	–0.09	0.10

4.2. Age

Using stellar effective temperature together with the absolute magnitude based on the Hipparcos parallax approximate stellar age can be interpolated according to [Fe/H] and [α/Fe] from theoretical stellar evolution tracks.

In this work we adopt the Yonsei-Yale isochrones (Yi et al. 2003), which are calculated with new OPAL opacities and Kurucz model atmospheres for a set of metallicities Z = 0.00001, 0.0001, 0.0004, 0.001, 0.004, 0.007, 0.01, 0.02, 0.04, 0.06, 0.08, and [α/Fe] = 0.0, 0.3, 0.6. The full set of stellar models and a FORTRAN package that works for metallicity and α-enhancement interpolation are available from the authors. We used different α-enhancement for sample stars according to our determinations.

4.3. Population membership

The identification of the population membership of a individual star is difficult. There are essentially two ways: the pure kinematical approach (e.g. Bensby et al. 2003, 2005) or by looking at a combination of kinematics, abundances, and stellar ages (e.g. Fuhrmann 1998, 2004).

In this work, we first calculated the relative probabilities for the thick-disk-to-thin-disk (TD/D) and thick-disk-to-halo (TD/H) membership using a method described by Bensby et al. (2003, 2005). The population definition was mainly based on the probabilities, but there are two exceptions: HD 108076 and HD 215257 have intermediate membership probabilities. HD 108076 was re-defined to thick disk star according to its age and α-element abundance, and HD 215257 to thin disk star according to its youth and α-element abundance.

Famaey et al. (2005) identified several kinematical subgroups in a local sample of giants, representative of the solar neighbourhood. Among them, the Hercules stream is crucial because its motion can be confused with that of the thick disk. We have computed each star's probability as belonging to the

Table 5. Kinematic properties, age, and population membership of sample stars.

Name	U [km s^{-1}]	V [km s^{-1}]	W [km s^{-1}]	$R_{\rm max}$ [kpc]	$R_{\rm min}$ [kpc]	$Z_{\rm max}$ [kpc]	e	[α/Fe]	Age [Gyr]	TD/D	TD/H	Pop.
HD 3454	–29.4	23.5	–23.5	11.0	8.2	0.3	0.15	0.16	7.7	0.05	>999.	thin
HD 6834	–1.4	22.0	–21.1	10.4	8.5	0.3	0.10	0.15	5.5	0.03	>999.	thin
BD+29 366	–50.7	–71.9	–39.2	8.9	4.3	0.6	0.35	0.27	20.0	14.59	>999.	thick
HD 18768	–76.5	41.6	–12.6	14.5	7.7	0.2	0.31	0.18	7.2	0.39	>999.	thin
HD 22879	–99.5	–80.5	–35.5	10.0	3.6	0.6	0.47	0.29	16.2	261.05	556.	thick
HD 25173	–78.0	–29.9	–8.0	10.1	5.7	0.1	0.28	0.17	7.6	0.11	>999.	thin
HD 28474	–4.2	10.9	48.8	9.7	8.5	0.8	0.07	0.20	17.0	0.42	>999.	thin
HD 45205	–74.5	–59.4	45.9	9.6	4.6	0.8	0.35	0.29	14.2	20.76	>999.	thick
HD 49732	40.6	32.3	–15.6	12.1	8.1	0.2	0.20	0.18	7.0	0.07	>999.	thin
HD 59374	–45.5	–119.3	0.3	8.7	2.4	0.0	0.56	0.29	17.6	>999.00	233.	thick
HD 59984A	–19.6	–44.1	–9.8	8.6	5.6	0.1	0.21	0.22	8.5	0.05	>999.	thin
HD 62301	7.2	–103.5	–16.7	8.5	3.0	0.2	0.47	0.23	11.5	124.04	644.	thick
HD 64385	27.7	–65.9	68.6	8.7	4.8	1.4	0.29	0.30	13.9	560.29	668.	thick
HD 76932	–36.4	–83.4	77.1	8.8	4.1	1.7	0.37	0.33	13.0	>999.00	213.	thick
HD 94028	–23.7	–134.8	16.7	8.6	2.0	0.2	0.63	0.28	19.4	>999.00	85.	thick
HD 101606A	–60.3	–19.1	19.6	9.8	6.4	0.3	0.21	0.19	3.9	0.06	>999.	thin
HD 105755	46.5	–3.3	–20.6	9.8	7.3	0.3	0.15	0.25	14.0	0.03	>999.	thin
HD 106516A	63.4	–67.3	–53.3	9.2	4.5	1.0	0.35	0.28	7.4	96.82	903.	?
HD 108076	–83.5	–37.4	–9.4	10.1	5.3	0.1	0.31	0.26	17.2	0.23	>999.	thick
HD 114762	–72.5	–64.3	62.1	9.5	4.6	1.3	0.35	0.27	14.1	477.67	626.	thick
HD 157089	–158.2	–37.6	–1.9	13.7	4.5	0.0	0.50	0.28	12.5	43.64	740.	thick
HD 189558	85.7	–122.3	50.1	9.4	2.3	1.0	0.60	0.33	10.8	>999.00	50.	thick
HD 194598	–65.6	–273.5	–21.7	8.9	1.0	0.3	0.79	0.22	13.2	>999.00	0.	halo
HD 195633	–49.6	–17.2	–2.9	9.5	6.6	0.0	0.18	0.16	6.2	0.02	>999.	thin
HD 200580	110.7	–63.4	11.8	10.6	4.1	0.2	0.44	0.20	8.8	11.07	>999.	?
HD 201889	–119.9	–79.4	–28.1	10.7	3.6	0.4	0.50	0.33	17.2	408.78	453.	thick
HD 204155	–24.5	–121.4	–36.1	8.6	2.4	0.5	0.56	0.28	12.3	>999.00	149.	thick
HD 207978	23.2	19.3	0.3	10.4	8.3	0.0	0.12	0.18	5.4	0.02	>999.	thin
HD 215257	–55.3	20.2	53.1	11.9	7.8	1.1	0.21	0.17	11.2	2.78	>999.	thin
HD 216385	–48.6	–3.2	–25.0	9.9	7.3	0.3	0.16	0.14	3.5	0.05	>999.	thin
HD 219617	396.4	–317.9	–65.0	58.9	1.6	4.8	0.95	0.36	11.7	>999.00	0.	halo
HD 221377A	–32.7	11.1	–21.6	10.1	8.0	0.3	0.12	0.25	4.6	0.03	>999.	thin

Hercules stream and find this probability to be low, i.e. all stars are disk or halo stars.

Finally, 14 stars were defined as thin disk stars, 14 as thick disk stars and 2 as halo stars. Of the remaining stars, HD 200580 recently was identified as a visual binary with an angular distance of the two stellar components of only 0.13 arcsec (Mason et al. 2001), and HD 106516 is a single-lined spectroscopic binary and a blue straggler candidate (Fuhrmann 2004). Table 4 gives the kinematic properties, age, α-elements abundance, and population membership for the sample stars. In Fig. 2 the kinematic status of our sample stars was shown in the Toomre diagram, while all our sample stars are consistent with the Fuhrmann (1998, 2004) definition. Figure 3 shows that thick disk stars have smaller $R_{\rm min}$, the minimum distance in stellar orbit, than thin disk stars, so it is another feature to use in identifying thin and thick disk stars.

Stellar age is a key feature for identifying stellar populations. For all our thick disk stars, stellar age is larger than 10.0 Gyr and the average is 15.0 ± 2.8 Gyr. For comparison, the average age of thin disk stars is 7.8 ± 3.7 Gyr. However, the average ages of the thin and thick disk stars given here are the results of our mildly metal-poor samples, but the metallicity distributions of the thin and thick disks peak at different metallicities, so our sample probably includes many old thin disk stars.

5. Discussion

The element-to-iron ratio of each element is plotted as a function of [Fe/H] in Fig. 4. The discussions are given in the following subsections.

5.1. α-elements (Mg, Si, Ca, Ti)

Both the quality of the spectra and the abundance analysis method of Chen et al. (2000) are similar to our work and the results of two works agree closely (see Table 4). In Fig. 5 we plot α-element abundances [α/Fe], which is defined as the average abundance of Mg, Si, Ca, and Ti with respect to the Fe of the two works. The population definition of the sample stars of Chen et al. (2000) was made by using same method as in this paper.

As seen in Figs. 4 and 5, the α-elements abundances of thin and thick disk stars show distinct abundance trends at [Fe/H] ≤ -0.60. The value of [α/Fe] in the thick disk stars

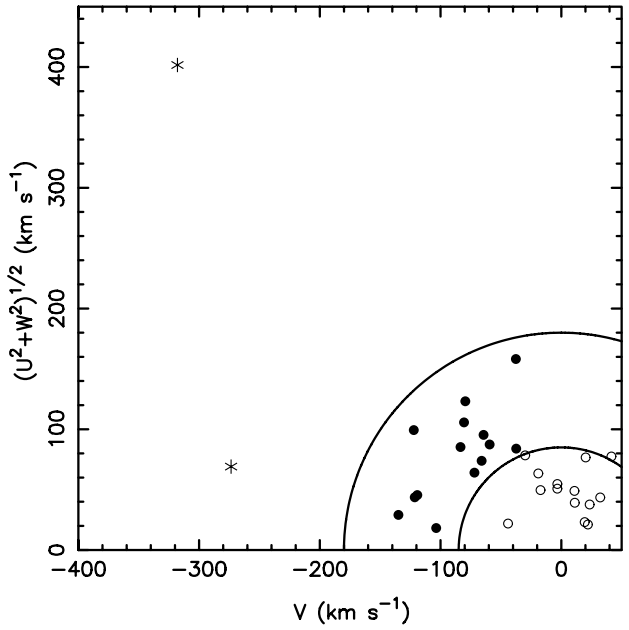

Fig. 2. Toomre diagram for the sample stars. Thin disk stars are denoted by open circles, thick disk stars are filled circles, halo stars are asterisk. The two circles delineate constant total space velocities with respect to the LSR of $V_{\rm tot}$ = 85 and 180 km s^{-1}, respectively, as used by Fuhrmann (2004) to define a sample of thick disk stars.

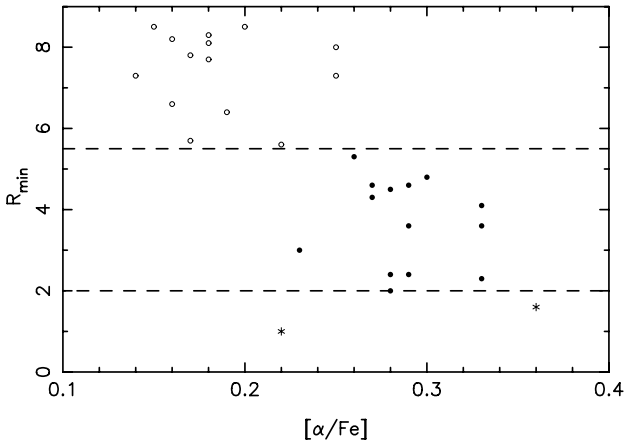

Fig. 3. $R_{\rm min}$ versus [α/Fe] for different populations. Symbols are the same as in Fig. 2.

remains constant at a level of about +0.3 dex, whereas [α/Fe] in the thin disk stars shows an increasing trend with decreasing [Fe/H] and reaches thick disk values at [Fe/H] ~ -0.80. However, we noted a small overlap in [Fe/H] between our thin and thick disk sample stars, so the abundance trends must be checked in thick disk stars with higher [Fe/H] and thin disk stars with lower [Fe/H].

For our two halo stars, [α/Fe] of HD 194598 is +0.22 ([Fe/H] = −0.99), lower than thick disk stars, and HD 219617 is +0.36 ([Fe/H] = −1.42), similar to thick disk stars and to the characteristic halo values.

The result is consistent with previous works. Fuhrmann (1998, 2004) found the thin and thick disks to be chemically distinct for the Mg element. Bensby et al. (2003, 2005) showed that [α/Fe] in the thick disk stars is constant at [Fe/H] ≤ -0.40, Above [Fe/H] = −0.40, [α/Fe] declines and the two disks merge together. Soubiran & Girard (2005) and Brewer & Carney (2005) also found similar behaviour.

This behaviour is interpreted as being due to the time delay between the type II SNe and long-lived type Ia SNe in the enrichment of the interstellar medium. Hence, star formation in the thick disk went on long enough that type Ia SNe started to enrich the gas out of which subsequent generations of thick disk stars formed.

It should be kept in mind that the population definition in most works has only been based on stellar kinematics; whether the thick disk stars with [Fe/H] ≤ -0.4 are true thick disk stars or contamination of thin disk stars needs further study. As pointed out by Gehren et al. (2004, 2005), the combination of stellar kinematics, age, and abundance makes the individual discrimination between stars of the different populations possible.

5.2. Oxygen

Oxygen is also an α-element that only forms in the interiors of massive stars through hydrostatic burning of mainly He, C, and Ne. Because oxygen is, next to hydrogen and helium, the most abundant element in the Universe, its abundance has extra importance for models of Galactic evolution. We discuss oxygen abundance in a separate section.

The determination of oxygen abundance is often troublesome. The two sets of features most often used for oxygen abundance determinations are two forbidden [O I] lines at 6300 and 6363 Å and the permitted high-excitation O I triplet in the 7771−7775 Å region. The formation of the [O I] lines is described well by LTE calculations, but the lines are weak in the spectra of metal-poor solar-type dwarfs. On the other hand, O I triplet lines are strong in the metal-poor stars; however, the lines are known to be very sensitive to effective temperature and NLTE effects (see e.g. Kiselman 1991). In recent years there has been a lot of work on O I NLTE analysis (e.g. Gratton et al. 1999; Asplund 2004; Takeda & Honda 2005).

Our oxygen abundances are based on the O I triplet lines, which give systematically higher abundances than do forbidden lines. We use Eqs. (1) and (2) of Bensby et al. (2004) to scale the oxygen abundances derived from the triplet to those derived from the forbidden [O I] line.

As seen in Fig. 4, the oxygen abundances of thin and thick disk stars also show distinct abundance trends, which agrees well with what we found for other α-elements (Mg, Si, Ca, and Ti).

Our result shows that [O/Fe] for thick disk stars with [Fe/H] < -0.6 is nearly constant, although the dispersions are large. Bensby et al. (2004) present oxygen abundances for a large sample of stars. They find distinctly different oxygen trends in the thin and thick disks; at [Fe/H] < -0.4 the [O/Fe] trend is nearly flat for thick disk stars, but the results of an extended sample (Bensby et al. 2005) show an increasing trend with decreasing metallicity. Jonsell et al. (2005) and Soubiran & Girard (2005) also find that [O/Fe] possibly increases

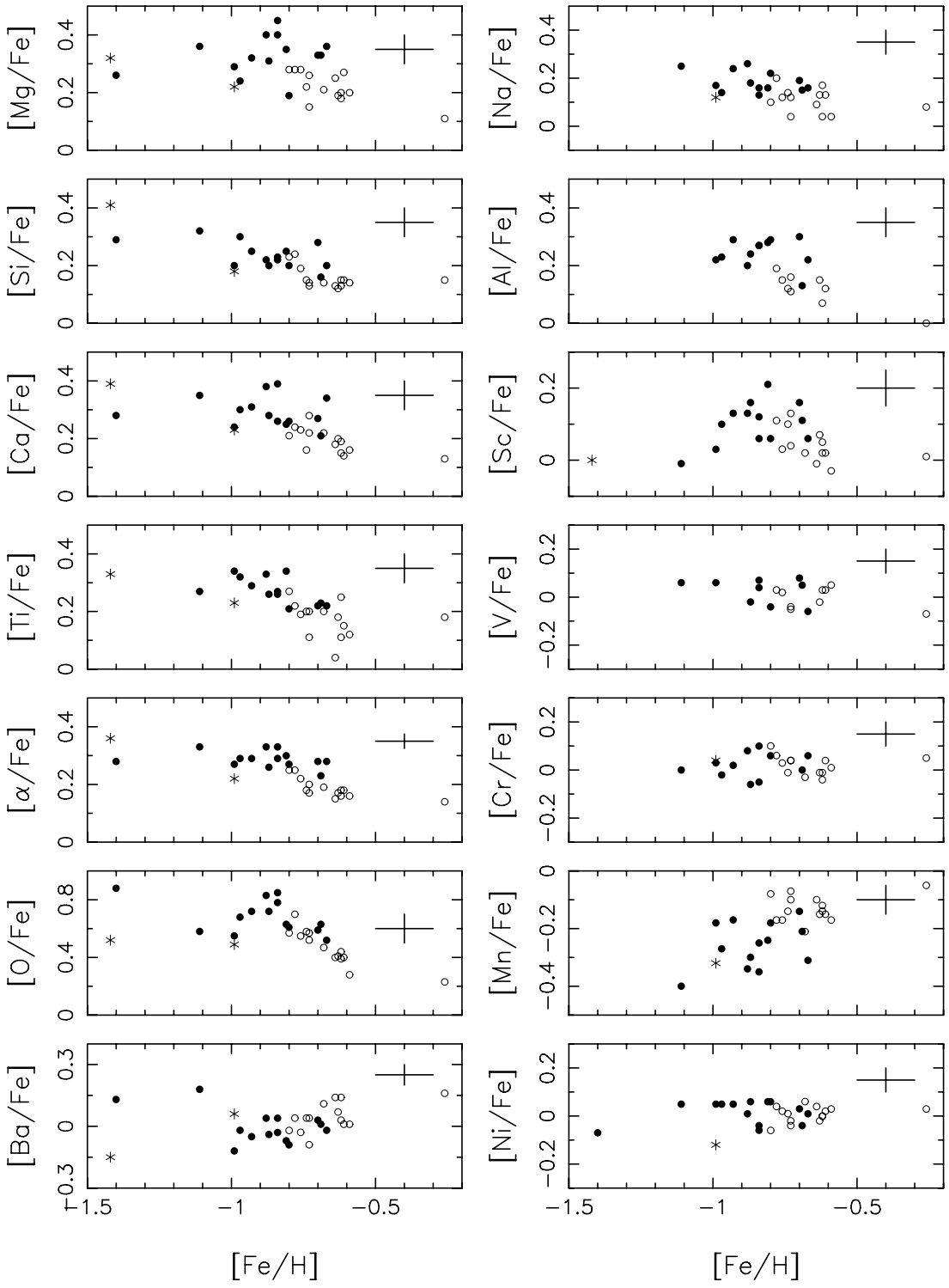

Fig. 4. Abundance patterns. The symbols are the same as in Fig. 2.

beyond [Fe/H] = −1.0. The behaviour is different from other α-elements (Mg, Si, Ca, and Ti). Bensby et al. (2004, 2005) also find different trends for oxygen compared to other α-elements at [Fe/H] > 0. The different behaviour between oxygen and other α-elements may reflect the nucleosynthesis process of these elements, Bensby et al. (2004) claim that oxygen is only produced in type II SNe. However, this conclusion remains tentative, because the NLTE and other effects make oxygen abundance determination with larger uncertainties as compared with other α-elements.

5.3. Sodium and aluminium

Both sodium and aluminium can be subject to NLTE effects. Our sodium abundances were determined from weak 6154/6160 lines. The NLTE calculation by Shi et al. (2004)

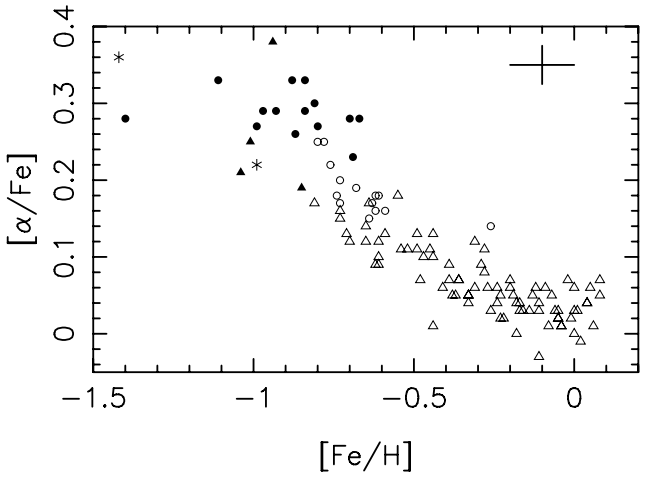

Fig. 5. The α-element abundance which is defined as the average abundance of Mg, Si, Ca, and Ti with respect to Fe of this work and in Chen et al. (2000). Thin and thick disk stars in Chen et al. (2000) are denoted by open and filled triangles, respectively. Symbols of stars in this work are the same as in Fig. 2.

shows 6154/6160 lines giving small NLTE effects (≤ -0.1 dex) for the disk dwarfs. The [Al/Fe] is slightly more affected by deviations from LTE, and the NLTE correction is $\sim$+0.2 dex for our sample stars (Gehren et al. 2004).

Both Na and Al are mainly produced during the C and N burning in massive stars, and they would therefore be ejected by SNe II, from a phenomenological point of view, so that Al and Na could be classified as mild α-elements. As shown in Fig. 4, [Al/Fe] behaves exactly like an α-element.

Our LTE sodium abundance trend is consistent with the NLTE result of Shi et al. (2004), although our [Na/Fe] systematically higher by 0.1 dex. If NLTE corrections are adopted, the differences will cancel.

Separation for [Na/Fe] of thin and thick disk stars is not quite as clear as seen for [α/Fe] and [Al/Fe]. The "merged" appearance is also found by Bensby et al. (2003), but Bensby et al. (2005) find that Na of the thin disk stars seems to be more abundant than the thick disk stars. Brewer & Carney (2005) find that the Na abundance remains near solar over the entire metallicity range for both the thin and thick disk stars, although the average thick disk abundance is slightly higher (0.04 dex) than that of the thin disk stars.

The NLTE study of Gehren et al. (2004, 2005) shows gradual decline of [Na/Mg] with [Mg/Fe] for thin and thick disk stars, but no such trend for [Al/Mg] with [Mg/Fe]. The comparison of [Na/Mg] and [Al/Mg] will help us to understand the nucleosynthesis process of these two elements, but it is still not clear, while the yields of both Na and Al in SNe II are under debate.

5.4. Iron-group elements

As seen from Fig. 4, among the iron-group elements, V, Cr, and Ni follow Fe very closely, and there is no offset between thin and thick disk stars.

Hyperfine structure (HFS) correction of Sc and Mn lines are significant, and our analysis adopts the hyperfine structure data of Prochaska & McWilliam (2000). Previous studies of Sc show different results. Zhao & Magain (1990) suggested that Sc was enhanced by $\sim$+0.25 dex in metal-poor stars. However, the result of Gratton & Sneden (1991) showed a solar ratio for [Sc/Fe]. Nissen et al. (2000) supports the high values of [Sc/Fe]. As seen from Fig. 4, [Sc/Fe] of thin disk stars shows a decreasing trend with increasing [Fe/H], thick disk stars with [Fe/H] > -1.0 have nearly constant value, [Sc/Fe] $\sim$ +0.15, but no significant enhancement at [Fe/H] < -1.0. Our [Sc/Fe] trend above [Fe/H] > -1.0 shows that Sc seems to follow the even-Z α elements like Mg, Si, Ca, and Ti; however, this similarity may not hold for stars with [Fe/H] < -1, which was also found by Prochaska & McWilliam (2000).

As seen from Fig. 4, there is a steplike change in [Mn/Fe] at [Fe/H] ~ -0.7. Thick disk stars with [Fe/H] ≤ -0.7 have [Mn/Fe] ~ -0.3, whereas thin disk stars with $-0.8 <$ [Fe/H] < -0.2 have [Mn/Fe] ~ -0.1. Nissen et al. (2000) published a detailed study of the trend of [Mn/Fe] in disk and metal-rich halo stars, but applied outdated data for the hyperfine structure of the Mn lines. Using modern hyperfine structure data, Prochaska & McWilliam (2000) found significant corrections to the [Mn/Fe] values of Nissen et al. (2000). Their revised data were plotted in Fig. 1.7 of Nissen (2003), and the [Mn/Fe] trend is very similar to our work. The trend of [Mn/Fe] almost mirrors that of [α/Fe] with respect to the [X/Fe] = 0 line, which suggests that type Ia SNe is a main source for the production of Mn.

5.5. Barium

Barium is thought to be formed during the main s-process that primarily occurs in low-mass AGB stars during He-shell burning. As shown in Fig. 4, the [Ba/Fe] of thin and thick disk stars also shows different behaviour. The slight declining trend of [Ba/Fe] with increasing metallicity for thick disk stars claimed by Mashonkina et al. (2003) is not clear in our LTE results, although [Ba/Fe] of two thick disk stars with [Fe/H] < -1.0 is larger than others with higher [Fe/H].

Bensby et al. (2005) found the [Ba/Fe] trends are different for the thin and thick disks. For the thick disk stars, the [Ba/Fe] is flat, lying on a solar ratio, though the thin disk [Ba/Fe] trend shows a prominent rise from the lowest [Fe/H] until reaching solar metallicities, after which it starts to decline. Reddy et al. (2003) found that [Ba/Fe] may be underabundant in thick disk stars relative to in thin disk. Brewer & Carney (2005) found that [Ba/Fe] is slightly enhanced in the thin disk stars compared to the thick disk stars for [Fe/H] < -0.2.

A series of very interesting papers on Ba abundance have been published by Mashonkina & Gehren (2000, 2001) and Mashonkina et al. (2003). Their results are obtained from NLTE differential analysis. Based on [Eu/Ba] ratio they estimate that the thick disk population formed on a timescale between 1.1 to 1.6 Gyr from the beginning of the protogalactic collapse.

6. Conclusion and future work

Chemical abundances of 14 elements for 32 mildly metal-poor stars were determined. According to kinematics, age, and

[α/Fe], stars were identified to the thin disk, thick disk, and halo population memberships. Element abundances for the different samples were discussed as a function of metallicities. The main results are summarized as follows:

1. The oxygen and other α-element (Mg, Si, Ca, and Ti) abundances of thin and thick disk stars show distinct trends at [Fe/H] ≤ -0.60.
2. For the odd-z elements, [Al/Fe] behaviour is exactly like an α-element, but separation for [Na/Fe] of thin and thick disk stars is not clear.
3. In the iron-group elements, V, Cr, and Ni follow Fe very closely, and there is no offset between thin and thick disk stars. The Sc and Mn abundance trends of the thin and thick disk stars are different.
4. The [Ba/Fe] of thin disk and thick disk stars shows different behaviour.

Our abundance, kinematics, and age results of a sample of mildly metal-poor stars confirm and extend previous studies of Galactic thin and thick disk stars.

Although there has been much effort in this field in the last decade, the abundance differences (e.g. α-elements) for the thin and thick disks stars are quite compelling, and one should note that most of the studies have selected stars with extreme kinematics to make it possible to classify stars as belonging to either the thin or thick disk populations. Thus, the conclusions may be affected by a kinematical bias. It is necessary to study large samples in a relatively homogeneous way.

It would be very interesting to make in situ studies of the abundances and kinematics for stars in the various places of the thin and thick disks. The Large sky Area Multi-Object fiber Spectroscopic Telescope (LAMOST project) of China, which combines a large aperture with a wide field of view and unprecedented multi-objects spectrographs, provides a good chance to study a huge number of thin and thick disk stars (Zhao et al. 2005). The large scale spectroscopic survey is expected to lead to major improvements in understanding the chemical and dynamical aspects of Galactic thin and thick disk populations and should lead to a model of Galactic formation and evolution.

Acknowledgements. This research is supported by the National Natural Science Foundation of China under grant number 10433010 and NKBRSF No. G1999075406. It made use of the SIMBAD database, operated at the CDS, Strasbourg, France.

References

Allen, C., & Santillan, A. 1991, Rev. Mex. Astron. Astrofis., 22, 255
Alonso A., Arribas, S., & Martinez-Roger, C. 1996, A&A, 313, 873
Asplund, M. 2004, A&A, 417, 751
Bensby, T., Feltzing, S., & Lundström, I. 2003, A&A, 410, 527
Bensby, T., Feltzing, S., & Lundström, I. 2004, A&A, 415, 155
Bensby, T., Feltzing, S., Lundström, I., et al. 2005, A&A, 433, 185
Brewer, M., & Carney, B. 2005 [arXiv:astro-ph/0509267]
Chen, Y. Q., Nissen, P. E., Zhao, G., Zhang, H. W., & Benoni, T. 2000, A&AS, 141, 491
Dehnen, W., & Binney, J. J. 1998, MNRAS, 298, 387
Edvardsson, B., Andersen, J., Gustafsson, B., et al. 1993, A&A, 275, 101
ESA 1997, The Hipparcos and Tycho Catalogues, ESA SP-1200
Famaey, B., Jorissen, A., Luri, X., et al. 2005, A&A, 430, 165
Fuhrmann, K. 1998, A&A, 338, 161
Fuhrmann, K. 2004, AN, 325, 3
Gehren, T., Liang, Y. C., Shi, J. R., Zhang, H. W., & Zhao, G. 2004, A&A, 413,1045
Gehren, T., Shi, J. R., Zhang, H. W., Zhao, G., & Korn, A. J. 2005, in preparation
Gilmore, G., & Reid, N. 1983, MNRAS, 202, 1025
Gratton, R. G., & Sneden, C. 1991, A&A, 241, 501
Gratton, R. G., Carreta, E., Eriksson, K., et al. 1999, A&A, 350, 955
Gratton, R. G., Carreta, E., Matteucci, F., et al. 2000, A&A, 358, 671
Johnson, D. R. H., & Soderblom, D. R. 1987, AJ, 93, 864
Jonsell, K., Edvardsson, B., Gustafsson, B., et al. 2005, A&A, 440, 321
Kiselman, D. 1991, A&A, 245, L9
Kurucz, R. L. 1993, CD-ROM No. 13, 18, Smithsonian Atrophysical Observatory
Majewski, S. R. 1993, ARA&A, 31, 575
Mashonkina, L., & Gehren, T. 2000, A&A, 364, 249
Mashonkina, L., & Gehren, T. 2001, A&A, 376, 232
Mashonkina, L., Travaglio, C., Gehren, T., et al. 2003, A&A, 397, 275
Mason, B. D., Hartkopf, W. I., Holdenried, E. R., et al. 2001, AJ, 121, 3224
Nissen, P. E., Chen, Y. Q., Schuster, W. J., & Zhao, G. 2000, A&A, 353, 722
Nissen, P. E. 2003, Origin and Evolution of the Elements, ed. A. McWilliam, & M. Rauch, Pasadena: Carnegie Observatories, Carnegie observatories Astrophys. Ser., 4, http://www.ociw.edu/ociw/symposia/series/symposium4/proceedings.html
Nissen, P. E., Chen, Y. Q., Asplund, M., et al. 2004, A&A, 415, 993
Reddy, B. E., Tomkin, J., Lambert, D. L., et al. 2003, MNRAS, 340, 304
Prochaska, J. X., & McWilliam, A. 2000, ApJ, 537, L57
Prochaska, J. X., Naumov, S. O., Carney, B. W., et al. 2000, AJ, 120, 2513
Shi, J. R., Gehren, T., & Zhao, G. 2004, A&A, 423, 683
Soubiran, C., & Girard, P. 2005, A&A, 438, 139
Takeda, Y., & Honda, S. 2005, PASJ, 57, 65
VandenBerg, D. A., Swenson, F. J., Rogers, F. J., et al. 2000, ApJ, 532, 430
Yi, S. K., Kim, Y. C., & Demarque, P. 2003, ApJS, 144, 259
Zhang, H. W., & Zhao, G. 2005, MNRAS, 364, 712
Zhao, G., & Li, H. B. 2001, ChJAA, 1, 555
Zhao, G., & Magain, P. 1990, A&A, 238, 242
Zhao, G., Chen, Y. Q., Shi, J. R., et al. 2005, ChJAA, submitted